

Direct Simulations of Particle Acceleration in Fluctuating Electromagnetic Field across a Shock

Takayuki Muranushi and Shu-ichiro Inutsuka

*Department of Physics, Kyoto University, Sakyo-ku, Kyoto, 606-8502, Japan;
muranushi@tap.scphys.kyoto-u.ac.jp*

ABSTRACT

We simulate the acceleration processes of collisionless particles in a shock structure with magnetohydrodynamical (MHD) fluctuations. The electromagnetic field is represented as a sum of MHD shock solution ($\mathbf{B}_0, \mathbf{E}_0$) and torsional Alfvén modes spectra ($\delta\mathbf{B}, \delta\mathbf{E}$). We represent fluctuation modes in logarithmic wavenumber space. Since the electromagnetic fields are represented analytically, our simulations can easily cover as large as eight orders of magnitude in resonant frequency, and do not suffer from spatial limitations of box size or grid spacing. We deterministically calculate the particle trajectories under the Lorentz force for time interval of up to ten years, with a time step of ~ 0.5 sec. This is sufficient to resolve Larmor frequencies without a stochastic treatment. Simulations show that the efficiency of the first order Fermi acceleration can be parametrized by the fluctuation amplitude $\eta \equiv \langle \delta B^2 \rangle^{\frac{1}{2}} B_0^{-1}$. Convergence of the numerical results is shown by increasing the number of wave modes in Fourier space while fixing η .

Efficiency of the first order Fermi acceleration has a maximum at $\eta \simeq 10^1$. The acceleration rate depends on the angle between the shock normal and \mathbf{B}_0 , and is highest when the angle is zero. Our method will provide a convenient tool for comparing collisionless turbulence theories with, for example, observations of bipolar structure of super nova remnants (SNRs) and shell-like synchrotron-radiating structure.

Subject headings: acceleration of particles — methods: numerical — MHD — turbulence

1. Introduction

Cosmic rays have the spectrum of $dN/dE \sim 10^5 (E/\text{GeV})^{-2.6} \text{cm}^{-2} \text{sr}^{-1} \text{s}^{-1} \text{GeV}^{-1}$ up to the so-called knee-energy of 10^{15} eV. Cosmic ray propagation theories suggest $dN/dE \propto E^{-2}$ energy spectra at the cosmic ray acceleration sites (e.g. Strong et al. 2007).

The current description of cosmic ray acceleration up to knee energy (10^{15} eV) is the well known first-order Fermi acceleration (Axford et al. 1977; Bell 1978). In the first-order Fermi acceleration model, magnetic turbulence is an important agent for particle acceleration. Turbulence makes the particle momenta isotropic, thus portion of the particles cross the shock front many times. Expectation value of the kinetic energy after N_J times of shock crossing is $E(N_J) = E_0 (1 + h)^{N_J}$. On the

other hand, the probability for a particle to survive N_J shock crossing can be roughly estimated as $P(N_J) = (1 - p)^{N_J}$. This gives us the power-law spectrum of $dP/dE = E^{-(h+p)/h}$.

Ellison et al. (1996), Lucek & Bell (2000), and Bell & Lucek (2001) have done simulations to describe the self-consistent generation of turbulence, with approximations such as gyro-center approximation, random walk approximation, or lowering the dimension. On the other hand, the recent development of the particle-in-cell simulation has made it possible to describe the particle acceleration in electron-positron plasma self-consistently (e.g. Spitkovsky 2008).

In this letter, we propose an alternative approach to the simulation of cosmic ray acceler-

ation. We have calculated the motion of particles deterministically, solving the particles' cyclotron motion from Larmor radii of thermal particles ($\sim 10^9\text{cm}$) to that of knee energy particles ($\sim 10^{17}\text{cm}$). According to the theories, we assume turbulence spectrum in $\log k$ space. This allows us to cover a large dynamic-range of space and energy, which enables us a direct comparison of the accelerated cosmic ray spectra with the observations.

2. Numerical Scheme

2.1. Representation of Turbulence

Upstream and Downstream Regions In our method, the electromagnetic field and velocity field of a continuous region are given by

$$\mathbf{B}(t, \mathbf{r}) = \mathbf{B}_0 + \sum_j \mathbf{B}_{1,j} \exp i(\mathbf{k}_j \cdot \mathbf{r} - \omega_j t + \phi_j) \quad (1)$$

$$\mathbf{u}(t, \mathbf{r}) = \mathbf{u}_0 + \sum_j \mathbf{u}_{1,j} \exp i(\mathbf{k}_j \cdot \mathbf{r} - \omega_j t + \phi_j) \quad (2)$$

$$\mathbf{E}(t, \mathbf{r}) = -\frac{1}{c} \mathbf{u}(t, \mathbf{r}) \times \mathbf{B}(t, \mathbf{r}) \quad (3)$$

where the amplitude and the wavenumber of the j -th mode are

$$\mathbf{B}_{1,j} = (\mathbf{n}_1 + i\mathbf{n}_2) B_t \left(\frac{k_j}{k_{\max}} \right)^{P_t} \quad (4)$$

$$\mathbf{u}_{1,j} = \frac{v_A}{B_0} \mathbf{B}_{1,j} \quad (5)$$

$$k_j = k_{\min} \left(\frac{k_{\max}}{k_{\min}} \right)^{j/(N_m-1)} \quad (6)$$

$$\omega_j = \pm v_A |\mathbf{k}_j| + \mathbf{k}_j \cdot \mathbf{u} \quad (7)$$

and the initial phase of the j -th mode is ϕ_j .

Here P_t is the spectral index that reflects the nature of the turbulence and N_m is the total number of the modes ($j \in \{1, \dots, N_m\}$), $\mathbf{B}_{1,j}$ is the amplitude for each mode, \mathbf{k}_j is its wavenumber, and $\mathbf{n}_1, \mathbf{n}_2$ are two mutually perpendicular unit vectors that are perpendicular to k_j . We choose \mathbf{k}_j to be either parallel or antiparallel to \mathbf{B}_0 . Equation (6) means that k_i are logarithmically discrete.

We use $\eta = (\sum_j B_{1,j}^2)^{\frac{1}{2}} B_0^{-1}$ as the measure of the strength of the fluctuation, independent of N_m . Because increasing N_m while keeping $\eta = \text{const}$ (1) keeps the magnetic energy in fluctuation mode, and (2) keeps the expectation value of the fluctuation field $|\langle \sum_j \mathbf{B}_{1,j} \rangle|$ the same, if ϕ_j are independent. We will confirm these properties in section 3.

Table 1: Parameters Used for our Simulations

$u_{up} = 3.0 \cdot 10^8 \text{cms}^{-1}$	fluid speed in shock frame
$v_{Aup} = 1.0 \cdot 10^7 \text{cms}^{-1}$	Alfven speed in fluid frame
$B_{0up} = 1.0 \cdot 10^{-5} \text{G}$	unperturbed magnetic field strength
$B_{1up} = \eta B_{0up}$	torsional Alfven mode energy
θ	angle of \mathbf{B}_0 to shock normal
$\lambda_{\max} = 10^{17} \text{cm}$	maximum wavelength of turbulence
$\lambda_{\min} = 10^9 \text{cm}$	minimum wavelength of turbulence
$T = 0.24 \text{keV}$	temperature of the particles
$m = 1.6 \cdot 10^{-24} \text{g}$	particle mass
$e = 4.8 \cdot 10^{-10} \text{esu}$	particle charge

The argument to derive $P_t = -1/3$ in $\log k$ space is summarized below: Variables in $\log k$ space are marked by tilde. The power law energy spectrum is $E(k)dk \propto k^{-\frac{5}{3}}$ in Kolmogorov turbulence case. This energy spectrum is in linear bin. In log energy bin the spectral power is $\tilde{E}(k)d\log k \equiv kE(k)dk \propto k^{-\frac{2}{3}}$; and since $\tilde{E} = 1/(8\pi)\tilde{B}^2$, $\tilde{B}(k)d\log k \propto \tilde{E}(k)^{\frac{1}{2}}d\log k \propto k^{-\frac{1}{3}}$. Thus, we get $P_t = -1/3$ for our discretization of the turbulent magnetic field.

Junction Conditions We assumed strong shock junction condition with low plasma β limit at the shock front: $u_{dn} = J^{-1}u_{up}$, $B_{\parallel dn} = B_{\parallel up}$, and $\mathbf{B}_{\perp dn} = \mathbf{B}_{\perp up}J$, where J is the shock compression ratio, B_{\parallel} and \mathbf{B}_{\perp} are components of the \mathbf{B} normal and tangential to the shock, respectively.

2.2. Initial Condition and Equation of Motion

Initial Condition For each set of initial condition we introduce electromagnetic fields described in section 2.1. We choose a set of initial turbulence phase $\{\phi_j\}$, sign of \mathbf{k}_j and ω_j from uniform distribution. Then we put 10^5 protons in Boltzmann distribution of temperature T at the upstream side of the shock.

We use the values in Table 1, based on Bamba et al. (2003)'s observation of SN 1006.

Evolution We make each turbulence mode propagate at Alfven velocity of the uniform field $v_A = B_0/\sqrt{4\pi\rho}$ as in Equation 1 - 3, and updated the particle with Lorenz force, with 4-th order Runge-Kutta method. We choose time dis-

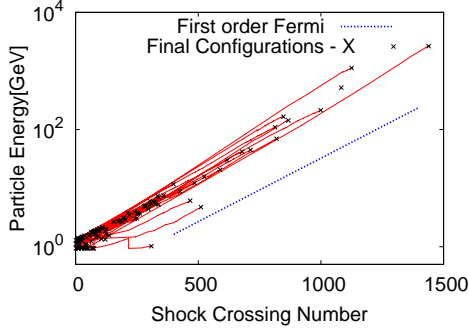


Fig. 1.— Particle energy as a function of number of shock crossing, after ~ 1 years of time evolution with parameters $\lambda_{\max} = 10^{17}$ cm, $\eta \equiv (\sum_j B_{1,j}^2)^{\frac{1}{2}} B_0^{-1} = 10$, and $\theta = 0$ (\mathbf{B}_0 is parallel to the shock normal). The red curves are particle trajectories and inclination of the blue line is the prediction of the first order Fermi acceleration theory.

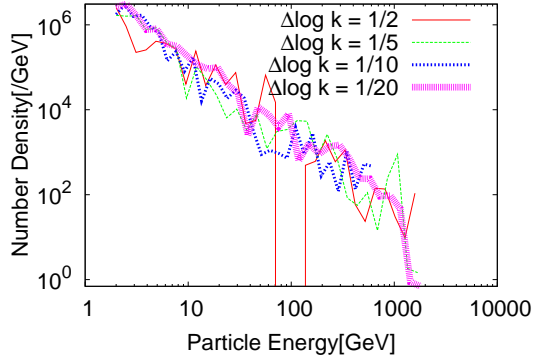


Fig. 2.— “Convergence” test for energy spectrum. Curves shows the particle energy spectrum at ~ 1 year time evolution. Each curve corresponds to discretization of the turbulence spectra into log k space with different $\Delta \log_{10} k$: number of modes per decade, while $\eta \equiv (\sum_j B_{1,j}^2)^{\frac{1}{2}} B_0^{-1} = 10$ is kept. Other parameters are $\lambda_{\max} = 10^{17}$ cm and $\theta = 0$. Particle with energy greater than 2GeV are counted.

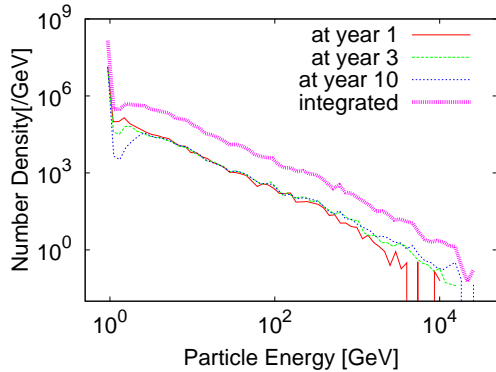


Fig. 3.— Curves show the particle energy spectra for $\lambda_{\max} = 10^{17}$ cm and $\eta = 10$, $\theta = 0$ at 1, 3, and 10 years of time evolution. Time integrated energy spectrum is shown with the bold curve.

cretization dt for each particle at every timestep, so that $dt < 0.1(1 + \eta)eB_0m^{-1}c^{-1}$ and $dt < 0.03e|\mathbf{B}_0 + \sum \mathbf{B}_1|m^{-1}c^{-1}$ always hold. Typical time step is 0.5s whereas the Larmor period of thermal particle for B_0 is $\sim 10^2$ s.

$$\frac{d\mathbf{r}}{dt} = \frac{\mathbf{p}}{\gamma m} \quad (8)$$

$$\frac{d\mathbf{p}}{dt} = e \left(\mathbf{E} + \frac{\mathbf{v}}{c} \times \mathbf{B} \right) \quad (9)$$

3. Result

We have made following examinations for the results of our method. First, we have traced the particles’ energy E as the function of shock crossing number N_J (Figure 1). The inclination of the curves match the inclination of the theoretical prediction, $E(N_J) = \{1 + (2/3)(v_{up} - v_{dn})/c\}^{N_J}$. Secondly, we have traced the spatial location where the particles gained their kinetic energy. We have found that 94% of the final kinetic energy have been earned within 1 final Larmor radius away from the shock. This is consistent with the first-order Fermi acceleration picture. Thirdly, we have studied the validity of our Fourier representation in log k space. We have kept the physical parameters and increased the number of modes per decade $\Delta \log_{10} k \equiv (N_{\text{mode}} / \log_{10})(k_{\max}/k_{\min})$; we see that the spectra converge, and converge to the theoretical power-law spectrum (Figure 2). This justifies our use of log k space discretization.

We have done a large number of simulations while varying the background conditions, λ_{\max} from 10^{13} cm to 10^{17} cm, η , the ratio of magnetic energy in fluctuation mode to that in background field from 0.3 to 300, θ , the angle between the background field and the shock normal from 0 to $\pi/2$. Figure 3 shows the time evolution of the energy spectrum for 10 years. The high-energy end of the spectrum gradually grows, and reaches 2.5×10^{13} eV by 10 years.

In our simulation all the particles start its motion in the given time. Since we don’t include the back-reaction from the particles to the electromagnetic field in our simulations, time-integral of energy spectra at each time-slice gives the steady state energy spectra. This steady state spectrum is also shown in Figure 3 with thick curve. The nonthermal component has $E(k) \propto k^{-1.6}$ power-

law spectrum that meets the observational requirement mentioned in section 1. We can also estimate the “injection rate” to be the proportion of particles that have more than 2GeV of energy after 1 years. For $T = 0.24\text{keV}$, 24keV , 2.4MeV , and 0.24GeV , the injection rate was < 0.001 , 1.9×10^{-2} , 8.4×10^{-2} , and 0.378 , respectively. The other parameters are $\eta = 30$, $\theta = 0$ and $\lambda_{\text{max}} = 10^{17}\text{cm}$.

In Figure 4 we show for all the parameter range the ratio of the particle numbers that were accelerated to have energy greater than 2GeV. We see that the acceleration is most efficient at polar region ($\theta \simeq 0$) when $\eta > 1$. We can understand this dependence of the spectra with background fluid parameters as follows; particles are trapped in Larmor motion and tend to move in direction of \mathbf{B}_0 . Thus particles more easily cross the shock-front when \mathbf{B}_0 is parallel to shock normal. If the turbulence amplitude is much weaker, fewer particles get reflected by pitch angle scattering, and Fermi acceleration is suppressed. The injection is more efficient for smaller λ_{max} , because more energy is distributed to modes with smallest wavelengths which are resonant with the thermal particles.

If a spherical shock emerges in a uniform mean magnetic field, there are two polar region where the mean magnetic field is parallel to the shock normal, and the equatorial region has the mean magnetic field perpendicular to the shock normal. Thus, we expect the Fermi acceleration process to be only active in the pair of polar region. This might explain the bipolar structure we see at SN 1006.

We have also checked the acceleration rate in three-dimensional(isotropic), rather than one-dimensional(anisotropic) distribution of \mathbf{k}_i . We have found that less significant dependence of injection rate on θ with larger η . We can interpret this as follows; if the turbulence spectrum is isotropic and the maximum turbulence wavelength is large, turbulence modes with largest wavelength and strongest amplitude play the role of local \mathbf{B}_0 . Thus we observe almost isotropic Fermi acceleration. This might explain the many SNRs with no typical orientation.

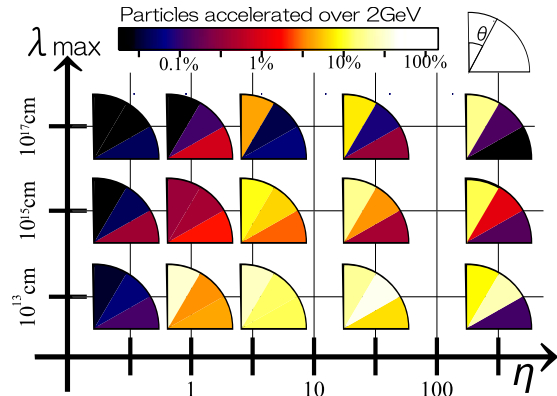


Fig. 4.— Parameter dependence of particle acceleration efficiency. λ_{max} is the longest wavelength of the turbulence modes, $\eta = (\sum_j B_{1,j}^2 B_0^{-2})^{\frac{1}{2}} \in \{0.3, 1, 3, 30, 300\}$ is the ratio of turbulent magnetic field to unperturbed magnetic field, θ is the angle between shock normal and \mathbf{B}_0 .

4. Discussion

Some might question the validity of η value much greater than unity. However, Uchiyama et al. (2007) observed extremely fast varying X-ray images at SNR RX J1713.7-3946. Their observation may indicate that magnetic field is locally enhanced up to 1mG in ~ 1 year in SNR, which corresponds to $\eta = 100$ case in our model. Our simulations suggest that such fast-varying spots in SNRs might be the sites of galactic ($E < 10^{15}\text{eV}$) cosmic ray acceleration.

Although we have ignored many of the Fourier modes by adopting $\log k$ space discretization of the turbulence spectrum, the validity of the approximation can be argued in many ways. Most importantly we have confirmed that our measure in $\log k$ space lead to convergence. Figure 2 shows energy spectra for $\eta = \text{const}$, with increasing $\Delta \log_{10} k$. Turbulent cascade, from which the very turbulence arises, is by nature a logarithmic process: a mode of a certain wavelength couples with the mode of half the wavelength by nonlinear term of Euler equation. First order Fermi acceleration also is a logarithmic process: particles gain energy as an exponential function of shock crossing number $E(N_J) = E_0 (1 + h)^{N_J}$. All these reason combined, waves in logarithmically discretized wavenumber space act as a sufficient ladder to

carry up cosmic ray particles.

The authors thank S. Inoue and K. Murase for useful comments. They also thank Center for Computational Astrophysics (CfCA) of National Astronomical Observatory of Japan and Yukawa Institute for Theoretical Physics (YITP) in Kyoto University for their computing facilities. The numerical calculations were carried out on Cray XT4 at CfCA and Altix3700BX2 at YITP. S. I. is supported by Grants-in-Aid (15740118, 16077202, and 18540238) from Ministry of Education, Culture, Sports, Science and Technology (MEXT) of Japan. This work was supported by the Grant-in-Aid for the Global COE Program "The Next Generation of Physics, Spun from Universality and Emergence" from the MEXT of Japan.

REFERENCES

- Axford, W., Leer, E., & Skadron, G. 1977, in International Cosmic Ray Conference, Vol. 11, International Cosmic Ray Conference, 132
- Bamba, A., Yamazaki, R., Ueno, M., & Koyama, K. 2003, *ApJ*, 589, 827
- Bell, A. 1978, *MNRAS*, 182, 147
- Bell, A., & Lucek, S. 2001, *MNRAS*, 321, 433
- Ellison, D., Baring, M., & Jones, F. 1996, *ApJ*, 473, 1029
- Lucek, S., & Bell, A. 2000, *MNRAS*, 314, 65
- Spitkovsky, A. 2008, *ApJ*, 682, L5
- Strong, A. W., Moskalenko, I. V., & Ptuskin, V. S. 2007, *Annual Review of Nuclear and Particle Science*, 57, 285
- Uchiyama, Y., Aharonian, F., Tanaka, T., Takahashi, T., & Maeda, Y. 2007, *Nature*, 449, 576